Supporting information

High-Strength, Self-Healing Conductive Polyurethane with Covalent Crosslinking and Reversible Dynamic Bonds for Multifunctional Strain Sensors

Zhecheng Hu [a, b, c, †], Changsheng Wang [a, b, c, †], Xiwei Xu [a, b, c],Ziqian Wang [a, b, c], Yuxuan Xie [a, b, c], Zequan Li [a, b, c, d, *], Wei Gao [a, b, c]

[a] *School of Resources, Environment and Materials, Guangxi University, Nanning 530004, Guangxi, China*

[b] *State Key Laboratory of Featured Metal Materials and Life-cycle Safety for Composite Structures, Guangxi University, Nanning 530004, China*

[c] *Guangxi Engineering and Technology Research Center for High Quality Structural Panels from Biomass Wastes, Nanning 530004, Guangxi, China*

[d] *Guangxi Key Laboratory of Petrochemical Resource Processing and Process Intensification Technology, Guangxi University, Nanning 530004, China*

[†] *These authors contributed equally to this paper.*

[*] *Email of corresponding author: zequan@gxu.edu.cn (ZQ Li)*

1. Chemicals and Solvents

N,N-dimethylacetamide(DMAc), Poly (tetramethylene ether glycol) (PTMEG, Mn = 2000 g mol^{-1}) Isophorone diisocyanate (IPDI, 99%), and Dibutyltin dilaurate (DBDTL, 95%) were purchased from Shanghai Aladdin Biotechnology Technology Co. Terephthalic dihydrazide (TD, 90%) was purchased from Anhui Senrise Technology Co. Hexamethylene diisocyanate isocyanurate trimer (tri-HDI) was purchased from Guangdong Yunxing Biotechnology Co. Super P was purchased from Tianjin Anuohe New Energy Technology Co. All reagents were used as received without further purification.

2. Sample Preparation

2.1. Synthesis of Self-healing polyurethane TDPU

The typical synthetic routes of TDPU polymers are shown in Fig S1 and described in detail below. In a three-necked round-bottomed flask equipped with a mechanical stirrer, 12 g of PTMEG (Mn = 2000 g mol^{-1}) was added. The mixture was then heated under a vacuum condition at 120 °C and stirred for 30 min to remove water. After cooling the reaction system to 80 °C, isophorone diisocyanate (IPDI, 2.667 g, 12 mmol) and dibutyltin dilaurate (DBTDL, 0.02 g), dissolved in N, N-dimethylacetamide (DMAc, 20 ml), were added to the flask. The reaction system was further heated and stirred at 80 °C for 4 h under N2 atmosphere and then cooled to 40 °C. 3,3'-Dithiodipropionic acid dihydrazide dissolved (DPH, 1.43 g, 6mmol)((Synthesis according to previous literature[1])) in DMAc (40 ml) and Terephthalic dihydrazide (TD, 1.165 g, 6 mmol) dissolved in DMAc (100ml) as a chain extender was added to the reaction system, which was continued to be heated and stirred at 40 ℃ for 10 h under N_2 atmosphere, and then the reaction system was heated up to 60 °C. Hexamethylene diisocyanate isocyanurate trimer (tri-HDI, 2.018 g, 4mmol) as crosslinking agent and dibutyltin dilaurate (DBTDL, 0.02 g), both were dissolved in DMAc (40 ml) was added to the reaction system. The reaction system was further stirred under a nitrogen atmosphere at 60 °C for 6 h. Finally, a viscous and transparent solution of TDPU polymers was obtained. The resulting polymer solution was poured into a glass petri dish, heated on a hot plate at 90 °C for 24 h, and then vacuum-dried at 80 °C for another 24 h to obtain the final polymer.

2.2. Preparation of flexible conductive elastomers (TDPU/SP-X%)

The solid content of the TDPU transparent solution was determined. Subsequently, varying amounts of vacuum-dried Super P conductive carbon black, dissolved in DMAc, were added to the TDPU transparent solutions. The system was then heated at 80 ℃ for 6 h. Finally, a viscous solution of TDPU/SP-X% was obtained, where X% represents the proportion of Super P to the total mass. The resulting polymer solution was poured into a glass petri dish, heated on a hot plate at 90 ℃ for 24 h, and subsequently vacuum-dried at 80 ℃ for an additional 48 h to obtain the final sample.

2.3. Preparation of Resistive Strain Sensors

The resistive strain transducer based on TDPU/SP-20% was fabricated into dimensions of 6.0 mm × 30.0 mm × 0.3 mm. Two copper wires, equipped with conductive tape at both ends, facilitated convenient measurements. The resistive strain sensors underwent uniaxial stretching and contraction, controlled by a stepper machine at a constant speed. The Keithley multimeter (Keithley 7510) was employed to monitor real-time resistance changes.

3. Physical Properties Characterizations

Infrared spectra were recorded by Fourier transform infrared equipped with attenuated total reflectance accessory

(ATR-FTIR, IRTracer-100). X-ray diffraction (XRD) patterns were recorded by an X-ray diffractometer Rigaku D/MAX 2500V with a scanning speed of 10°·min^{-1}. The Raman spectra were recorded in the range of 200-3000 cm^{-1} using a laser Raman spectrometer(inVia Reflex). Thermogravimetric analysis was carried out on a differential thermal-thermogravimetric analyzer (DTG-60H), the temperature range was 30-600 ℃, and the heating rate was 10 ℃·min^{-1}. The thermal performance analysis was carried out by differential scanning calorimeter (DSC), the temperature range was from -60 to 300 ℃, and the heating rate was 10 ℃·min^{-1}. Testing the electrical signal of resistive sensors with a Keithley multimeter (Keithley 7510).

4. Small-angle X-ray Scattering (SAXS) Measurements

The one-dimensional SAXS curves were integrated by averaging azimuthally 360° of 2D SAXS patterns via the Fit2D software. Micro-phase spacing(d) was calculated by the Bragg's law:

$$d = \frac{2\pi}{q_{max}}$$

where q_{max} corresponds to the peak position of one-dimensional SAXS curve.

5. Tensile Tests

All mechanical tests were conducted with a universal testing machine.

(1) The test specimens are cut into long dumbbell-shaped strips and fixed at both ends of the tensile clamping distance, with the initial clamping distance set at 14 mm and the stretching rate of 50 mm·min^{-1}. The true stress(σ) and elongation at break(ε) are calculated by the following equation:

$$\sigma = \frac{F}{b * d}$$

$$\varepsilon = \frac{L_{max} - L_0}{L_0} \times 100\%$$

Where σ is the tensile strength, F is the maximum tensile force that the film can bear before breaking, b is the width of the film, and d is the thickness of the film, ε is the elongation at break of the composite film, L_{max} is the distance between the clamps at the point of film breakage, and L_0 is the initial distance between the clamps for the composite film.

For cyclic tensile testing, the loading and unloading processes are carried out at a strain at a rate of 50 mm·min−1 at room temperature. In the first cyclic tensile experiment, the samples were subjected to ten consecutive cycles of unloading from 25% to 300% of stretch with no waiting time, with each strain incremented by 25%. In the second cyclic tensile experiment, the samples were subjected to ten consecutive unloading cycles of stretching up to 300% without waiting time.

(2) The toughness(τ) is defined as the area surrounded by the engineering stress (σ)-strain (ε) curves and calculated using the following equation:

$$\tau = \int_0^{\varepsilon_{max}} \sigma d\varepsilon$$

Where σ is the tensile strength of the sample, ε is the elongation of the sample and ε_{max} is the maximum elongation at break.

6. Self-Healing

Self-healing results were observed by optical microscopy.

7. Test Methods for Fracture Energy

Fracture energy was assessed using both unnotched and notched samples featuring a single notch with a length of 1mm. The specimens, whether unnotched or notched, measured 10.0 mm × 5.0 mm × 0.2 mm and underwent tensile testing at a speed of 3 mm min^{-1}. The fracture energy (Gc) can be determined using the following equation:

$$G_c = \frac{6wc}{\sqrt{\lambda_c}}$$

Where c represents the notched length (1 mm), λ_c represents the elongation at the break of the notched sample, and w represents the strain energy calculated by integrating the stress-strain curve of the unnotched sample up to ε_c.

8. Conductivity Testing Methods

Ion conductivity measurements were conducted using a circular sample membrane. The membrane, with a diameter of 16 mm, was placed between two stainless steel electrodes of the same diameter. The electrochemical workstation (CHI660E, Chenhua) measured the impedance spectrum (EIS) within the frequency range of 0.001 Hz to 1 MHz, with an amplitude of 10 mV. The ionic conductivity was calculated using the following equation:

$$\sigma = \frac{L}{RS}$$

where L represents the thickness of the circular sample, R represents the bulk resistance measured by EIS, and S represents the contact area of the sample membrane with the electrode.

To assess conductivity at various temperatures, EIS measurements were conducted across a temperature range from 30 ℃ to 110 ℃ with 10 ℃ intervals. Conductivity was then determined based on the EIS results.

The conductivity of TDPU/SP-X% was measured using a four−probe resistivity tester (Jandel RM3000), and the conductivity was calculated using the following equation:

$$\sigma = 1/K$$

where K represents the resistivity of the tested sample.

9. Statements

All human study participants provided informed written consent for the experiments.

Figure S1-S11

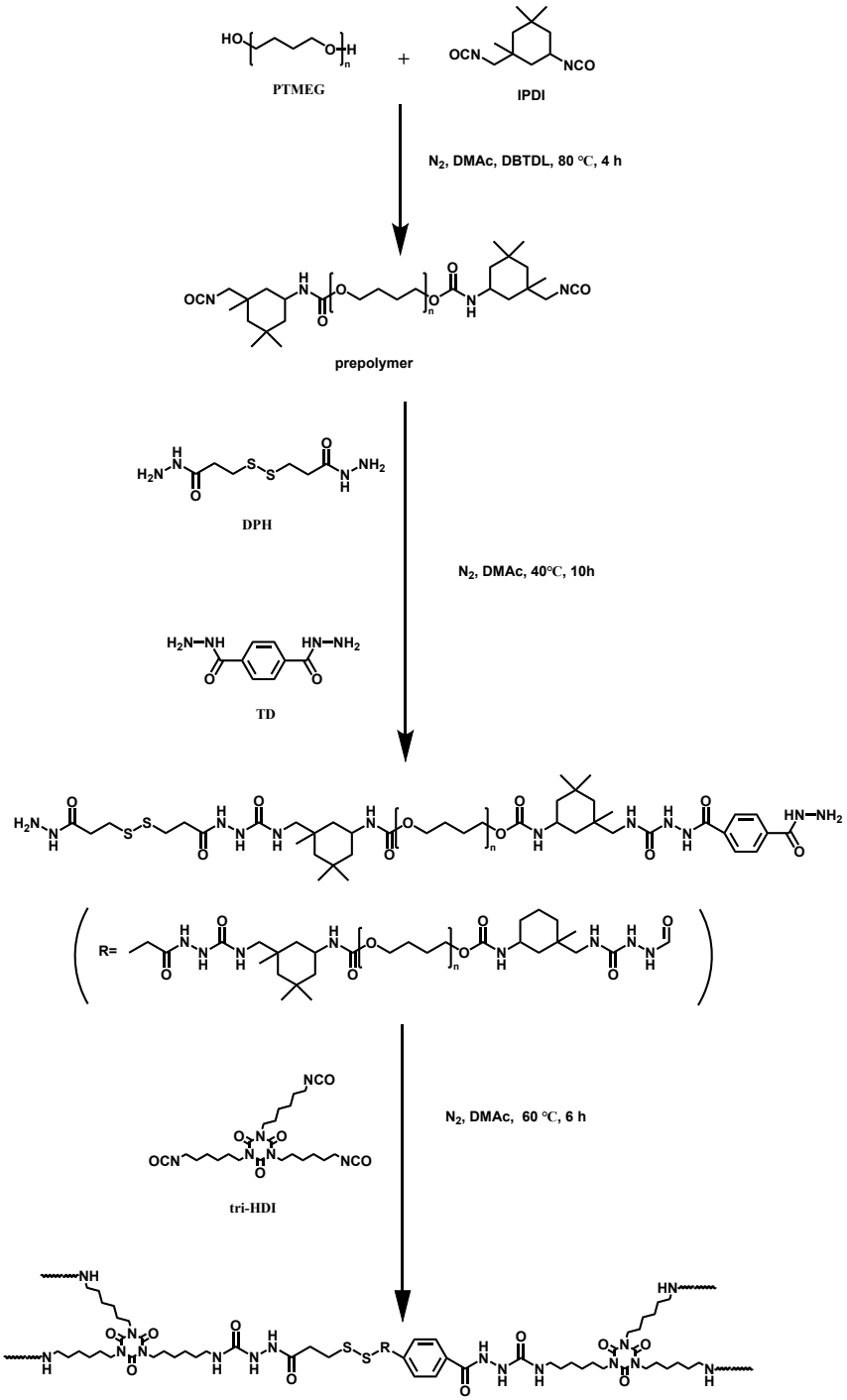

Fig S1. Synthesis routes of TDPU polymers.

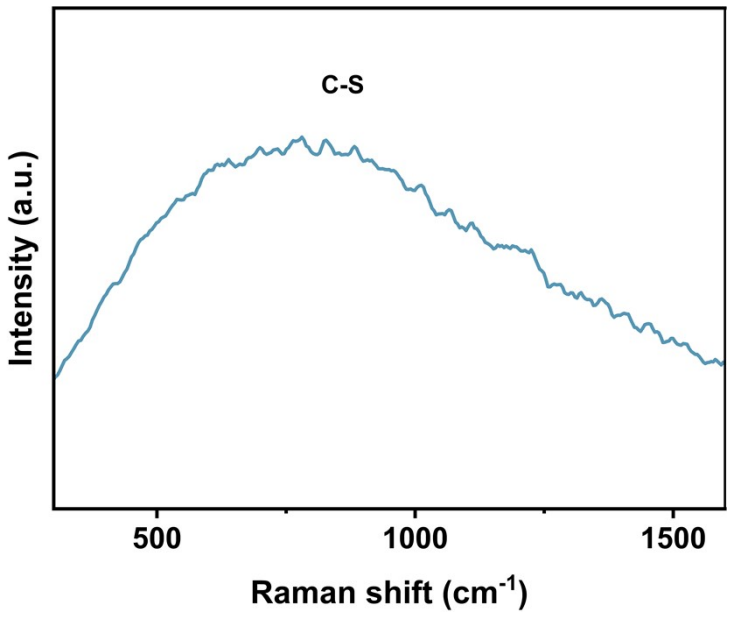

Fig S2. Raman spectra of TDPU/SP-0%.

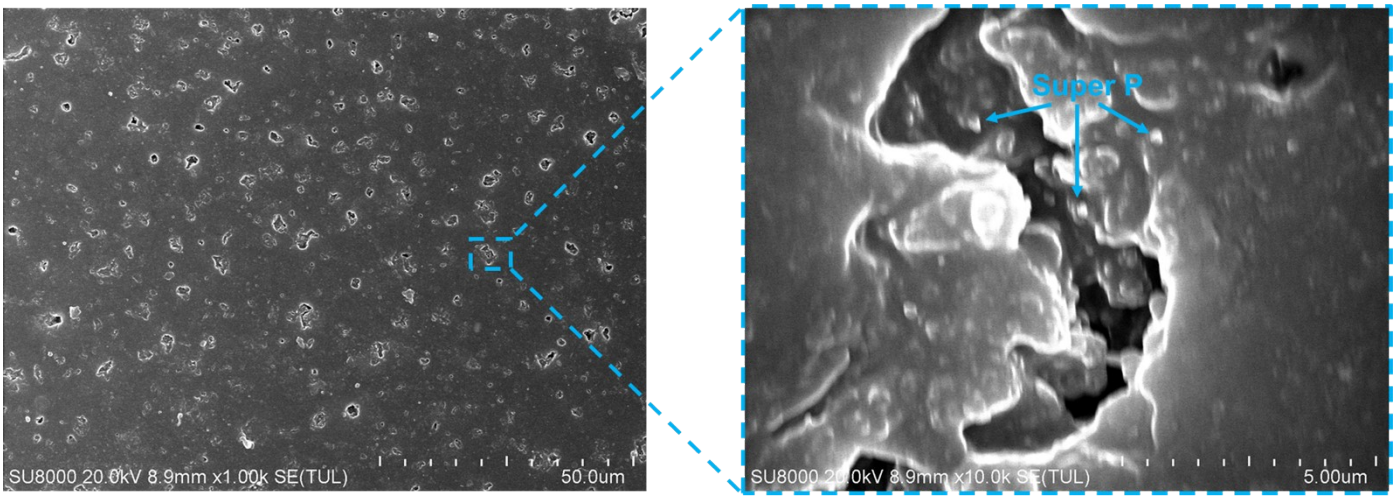

Fig S3. SEM micrographs of the TDPU/SP-20%.

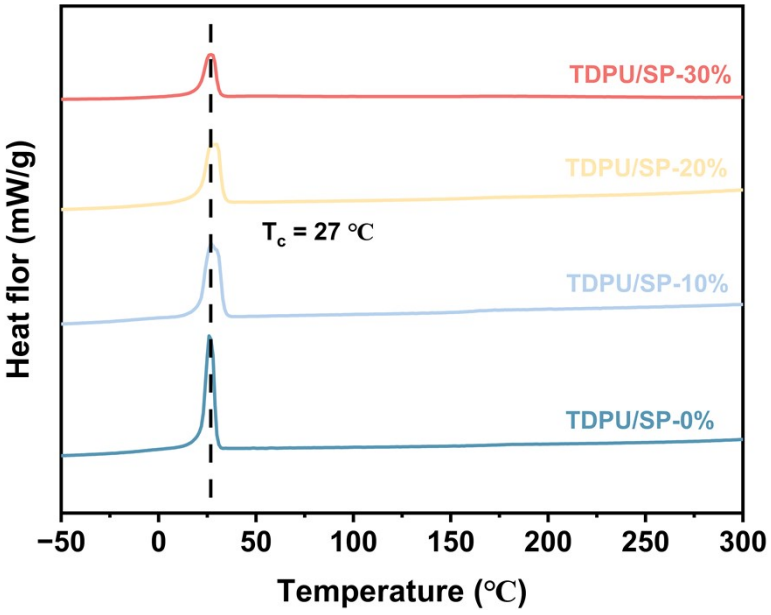

Fig S4. DSC tests of TDPU/SP-X%.

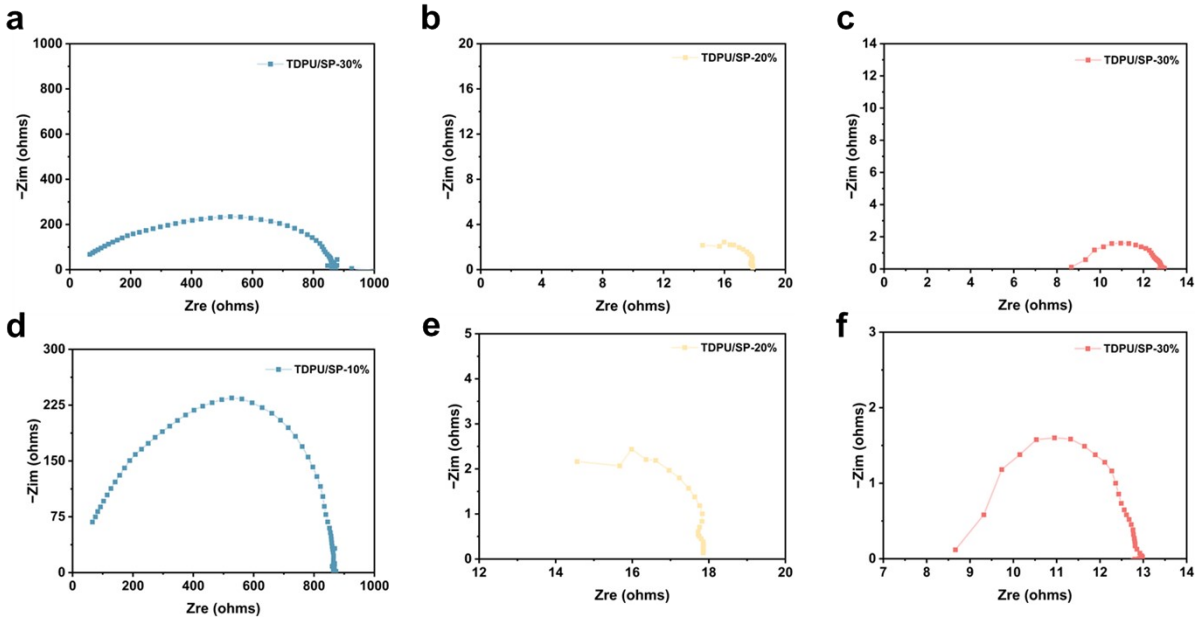

Fig S5. Electrochemical impedance spectra of (a) TDPU/SP-10%, (b) TDPU/SP-20%, (c) TDPU/SP-30%. Enlarge EIS of (d) TDPU/SP-10%, (e) TDPU/SP-20%, (f) TDPU/SP-30%.

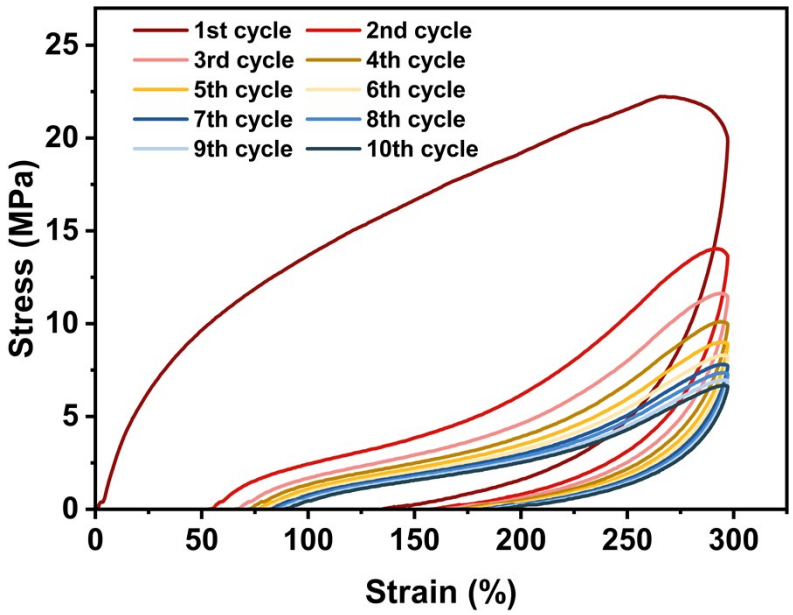

Fig S6. Results of cyclic tensile experiments on TDPU/SP-20% samples with 300% strain at 10 mm min^{-1}.

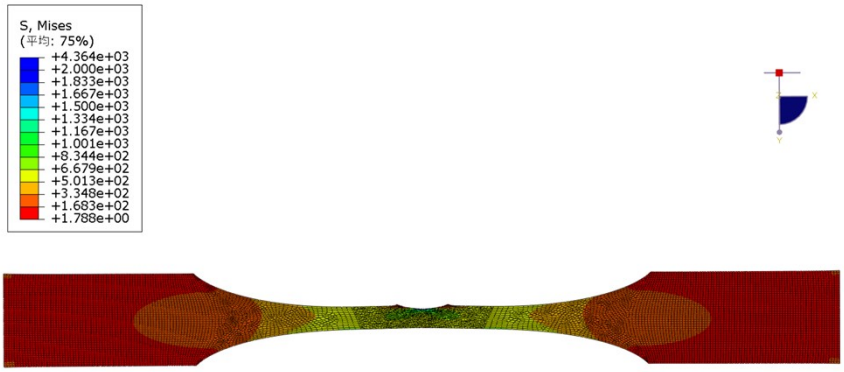

Fig S7. Finite element simulations on a sample of TDPU/SP-20%.

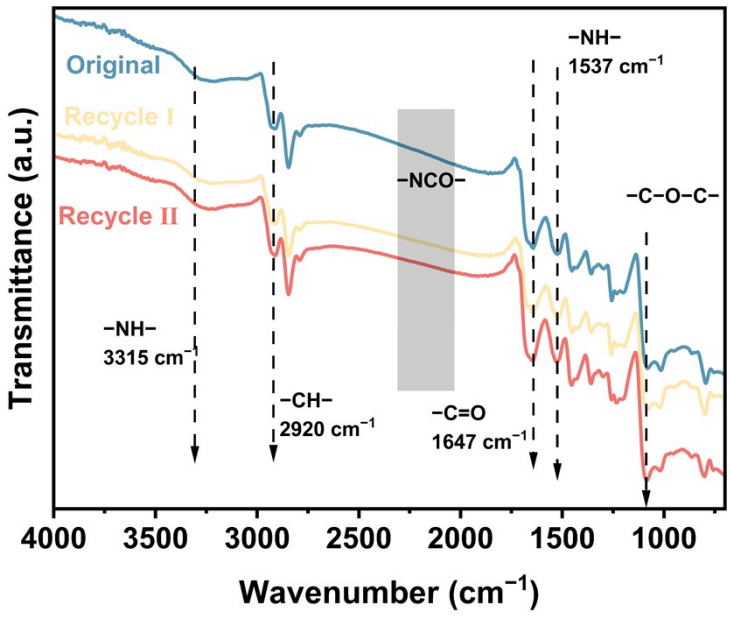

Fig S8. FITR test of TDPU/SP-20% after first hot-pressing recovery and second hot-pressing recovery.

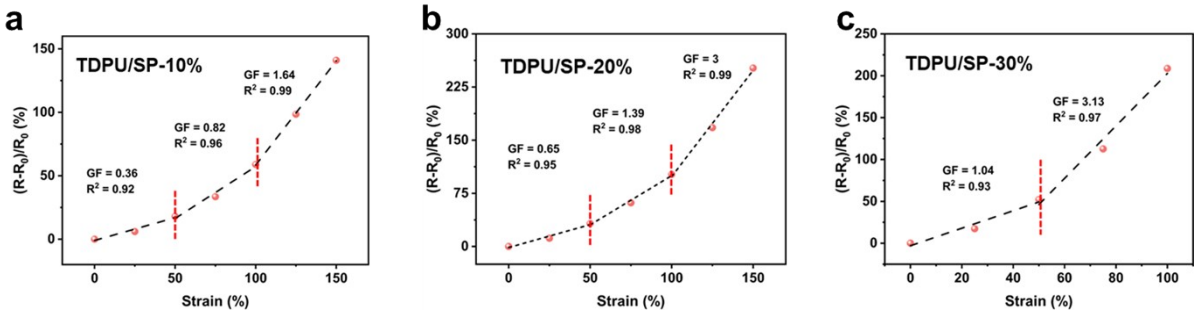

Fig S9. (a) DPU/SP-10%, (b)TDPU/SP-20% and (c) TDPU/SP-30% wearable sensors sensitivity tests.

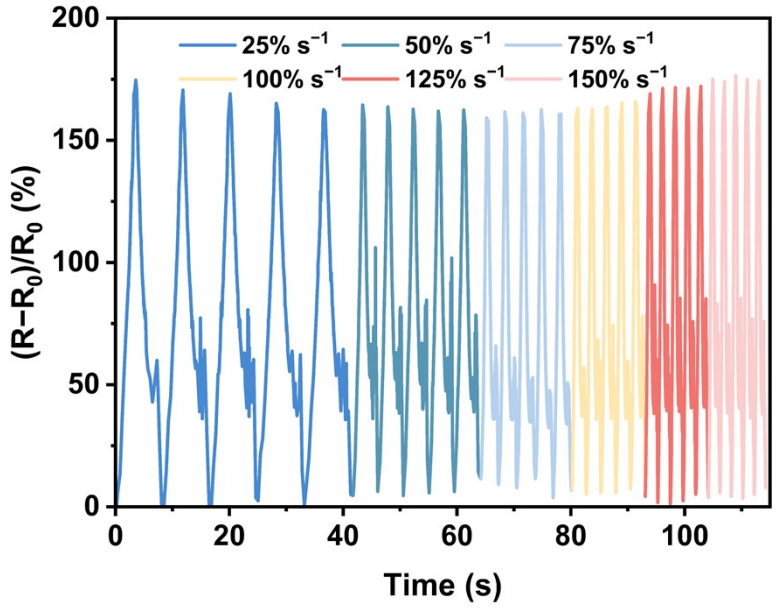

Fig S10. Relative resistance change of TDPU/SP-20% strain sensors at different strain rates (25-150%).

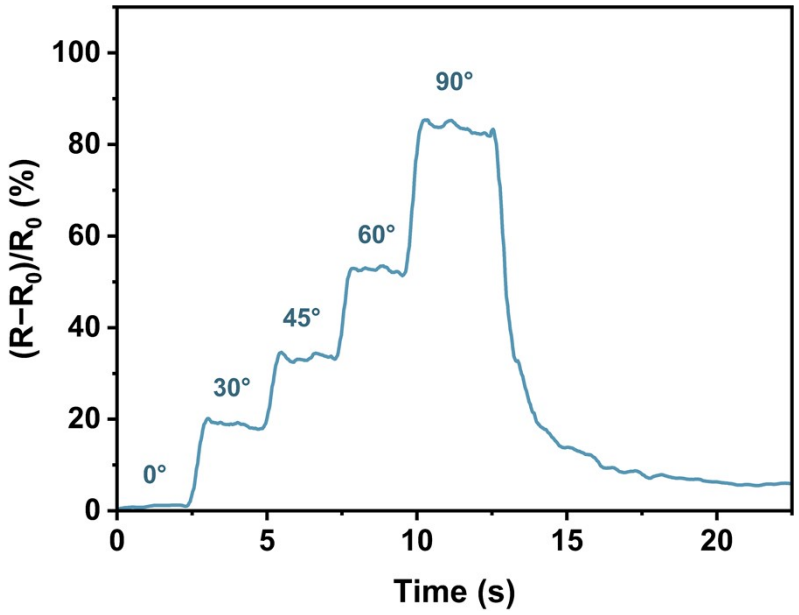

Fig S11. Relative resistance change of TDPU/SP-20% strain resistance sensors at different bending angles.

Table S1-S3

Table S1 Strength, stretchability, and toughness of TDPU/SP-X%.

Sample name	Carbon ratio (%)	Strength (MPa)	Stretchability (%)	Toughness (MJ m^{-3})
TDPU/SP-0%	0	38.42 ± 3.14	887	130.6 ± 7.42
TDPU/SP-10%	10	32.44 ± 2.81	623	113.30 ± 4.66
TDPU/SP-20%	20	27.87 ± 2.48	400	70.08 ± 4.95
TDPU/SP-30%	30	18.77 ± 2.10	145	19.75 ± 1.98

Table S2 Conductivity of TDPU/SP-10%, TDPU/SP-20%, TDPU/SP-30%.

Sample name	**Carbon ratio (%)**	**Conductivity (S cm^{-1})**
TDPU/SP-10%	10	$(3.60 \pm 0.85) \times 10^{-5}$
TDPU/SP-20%	20	$(2.35 \pm 0.64) \times 10^{-3}$
TDPU/SP-30%	30	$(3.30 \pm 1.41) \times 10^{-3}$

Table S3 Rough comparison of strength and conductivity of TDPU/SP-20% before and after recovery by hot pressing.

Sample name	**Carbon ratio (%)**	**Strength (MPa)**	**Conductivity (S cm^{-1})**
TDPU/SP-20%	20	27.87	$(2.35 \pm 0.64) \times 10^{-3}$
Reprocessing Ⅰ	20	26.56	$(1.40 \pm 0.34) \times 10^{-4}$
Reprocessing Ⅱ	20	11.56	$(7.00 \pm 1.32) \times 10^{-5}$

Movie S1-S2

Movie S1

The 6.0 mm × 30.0 mm × 0.3 mm specimen of TDPU/SP-20% successfully lifted a 2.5 kg weight.

Movie S2

Conducted crack extension tests on TDPU/SP-20% samples.

References

1. Z. Rodriguez-Docampo and S. Otto, *Chem. Commun.*, 2008, 5301-5303.